ISBN: 978-3-95450-262-2 ISSN: 2673-5350 doi: 10.18429/JACoW-IBIC2025-MOPMO07

FIRST Attila4MC SIMULATIONS FOR THE HIGH-POWER PROTON ACCELERATOR OF THE EUROPEAN SPALLATION SOURCE

E. Donegani*, European Spallation Source (ESS) Lund, Sweden

Abstract

Radiation transport simulations allow the design and operation of entire facilities such as the European Spallation Source (ESS) in Lund, Sweden. This paper summarizes three of the first applications of Attila4MC simulations to the high-power proton accelerator of ESS and its beam instrumentation. Entire linac sections and beam-interceptive instrumentation were modelled by implementing existing CAD models, relying on unstructured tetrahedral meshes and zeroing out the time spent in manually crafting MCNP6 models. As a result, it was possible to accurately quantify the beam power density within beam-interceptive devices and in turn their operational limits. Activation and 3D dose maps were computed and swiftly visualized in 3D, on top of the actual linac model. This work paves the way for e.g. advanced instrumentation design, linac operation, safe maintenance, categorization of radiation waste and future dismantling.

INTRODUCTION

The European Spallation Source (ESS) [1] in Lund (Sweden) will be the world's most powerful accelerator-based neutron source for groundbreaking science. The ESS accelerator will deliver 2.86 ms long proton pulses, at a repetition rate of 14 Hz with a proton current of 62.5 mA. The high current of protons in the [0.075, 2000] MeV range poses two main challenges: the beam power density and the radiation induced activation. Therefore, radiation transport simulations are necessary to compute the operational limits (for avoiding structural failures, melted components and quenches of superconducting sections), to map residual dose rates and to provide radionuclide inventories. In the past, radiation transport simulations of the ESS accelerator were performed with MCNPX [2], PHITS [3] and FLUKA [4]. In all cases, an extensive amount of time had to be invested to simplify CAD models and manually implement complex linac models. This paper presents for the first time the simulations of the ESS linac with Attila4MC [5], demonstrating the efficiency, versatility and accuracy of Attila4MC to speed up the simulation workflow, simulate linac components as-built and swiftly visualize computational meshes as well as the results directly on top of complex CAD models.

Attila4MC TO DEFINE THE OPERATIONAL LIMITS OF BEAM-INTERCEPTIVE DEVICES

Beam-interceptive devices in the ESS linac have to safely absorb and dissipate the high power of the ESS proton beam [6]. For example, the ESS MEBT Faraday cup [7] has to stop 3.6 MeV protons and measure the proton current (up to 62.5 mA). The most demanding beam modes are: the Fast Tuning (5 µs, 14 Hz) and the Slow Tuning (50 µs, 1 Hz). Besides the shallow Bragg peak of 3.6 MeV protons, the beam is typically Gaussian with σ_x and σ_y usually smaller than 5 mm. The key component of the ESS MEBT Faraday cup is its graphite collector that fully stops the proton beam.

No temperature sensor was integrated, because it would not quickly provide protection capabilities nor temperature measurements within the pulse duration. In addition, during the linac commissioning it was not possible to measure the actual size of the proton beam. Therefore, MCNP simulations coupled with thermomechanical calculations in ANSYS [8] were performed to foresee the operational limits. Attila4MC was the only software capable of computing the beam power density within the actual indented geometry, which could not be defined by means of the standard MCNP surfaces and macrobodies.

The Attila4MC results are swiftly visualized in 3D (see Fig. 1), with Tecplot [9], without the need to develop dedicated scripts for each different beam-interceptive device. The Attila4MC workflow for quantifying the beam power density starts by importing the CAD model in the Parasolid format (.x_t) into Attila4MC via ANSYS SpaceClaim [10]. The Unstructured Mesh (UM) is defined on top of the actual geometry of the ESS MEBT Faraday cup. The mesh is composed of first order tetrahedral elements, including 157589 node points and 736542 cells. The MCNP6.2 [11] input file (including materials, cross-sections, region attributes, MCNP controls and importances) is prepared via the GUI of Attila4MC. Protons, neutrons, electrons and photons are

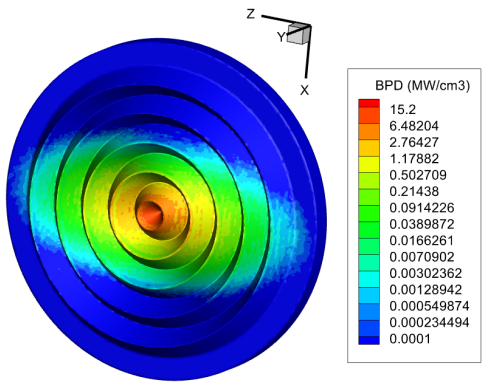

Figure 1: Beam Power Density (BPD) computed with Attila4MC within the graphite collector of the ESS MEBT Faraday cup. The collector has a radius of 29 mm and thickness of 8 mm. The 3.6 MeV protons beam is Gaussian with σ_x = 3 mm and σ_z = 5 mm; the proton current is 62.5 mA.

* elena.donegani@ess.eu

ISBN: 978-3-95450-262-2 ISSN: 2673-5350 doi: 10.18429/JACoW-IBIC2025-MOPMO07

transported. The ENDF70 libraries are used to compare the Attila4MC results with the MCNPX [12] results. The simulations ran on the DMSC cluster [13] until the statistical and convergence checks are passed. The UM serial processing took two hours and the actual particle transport with nps=10^8 took just 69 seconds, relying on 12 nodes (i.e. the DMSC Quark nodes, having 24 × 56 cores with 512 GB memory each). The MCNPX simulations for a flat collector with nps=10^9 ran for 21 hours, relying on three DMSC Newlong nodes, having 24 Dell FX430). The real gain by running Attila4MC is in the accuracy of the scientific results, as demonstrated in Fig. 2, comparing the Attila4MC results to the MCNPX results within a Structured Mesh (SM). In both cases, a Gaussian source of 3.6 MeV protons with $\sigma_x = \sigma_z$ was simulated. The SM results overestimate the BPD, leading to overly restricting operational limits, whereas the Attila4MC mesh preserves the actual geometry, mass and volume of the collector thus providing realistic BPD values.

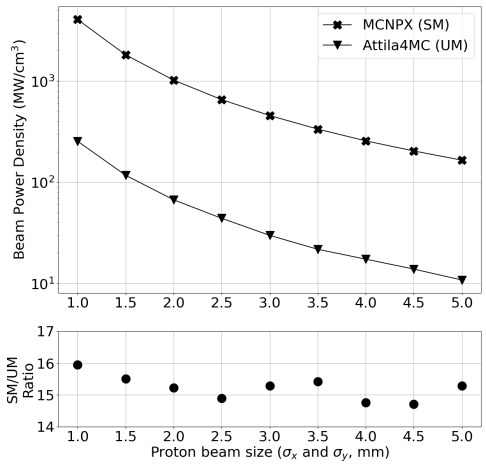

Figure 2: BPD results within a simplified flat collector and on top of the actual collector in the ESS MEBT Faraday cup.

Attila4MC FOR ADVANCED DETECTOR DESIGN AND ACTIVATION CALCULATIONS

The ESS accelerator is an extremely compact proton linac; its CAD model includes thousands of components (e.g. magnets, cryomodules, pipes, supporting structures and diagnostics devices). One of the main challenges is to design compact beam-interceptive devices [14] that not only safely withstand the high-power proton beam, but also fit in the limited space both inside and outside the beam pipe (see Fig. 3). In particular, beam-interceptive devices are directly exposed to protons and become radioactive following the release of secondary particles by the interactions of the primary protons within the device. Linac components in the vicinity of beam-interceptive devices become radioactive, too. Therefore, residual dose rates must be quantified in advance and be within the established radiation protection limits. Nuclide inventories are required by the authorities before granting operational licenses, dismantling processes and classification of any radioactive waste. Access to the linac components may be frequently needed during the linac commissioning e.g. for installation and maintenance.

Attila4MC allows to advance the design of beam-interceptive devices by starting from the actual CAD models of the linac to fully exploit the available space. In addition, Attila4MC allows to identify hotspots where accessibility and maintenance are severely limited due to enhanced radiation emission. For instance, Fig. 3 shows the activation results for the first SPK section in the ESS linac, hosting a beam stop [15] exposed to 100 MeV protons for one week at the average proton current of 1 µA. The input file was prepared with the Attila4MC GUI by defining materials, cross sections (SFSW-FENDL-31-FC), region attributes, energy group attributes, MCNP controls and importances. A bill of materials was used to speed up the material assignment in the various components. The meshing process can be accelerated by setting a volume threshold, thus skipping e.g. hundreds of screws.

The neutron flux was calculated in Attila4MC with an `f4` tally, using 53 neutron groups as required for the subsequent activation calculations in Fornax [16]. Once the calculations

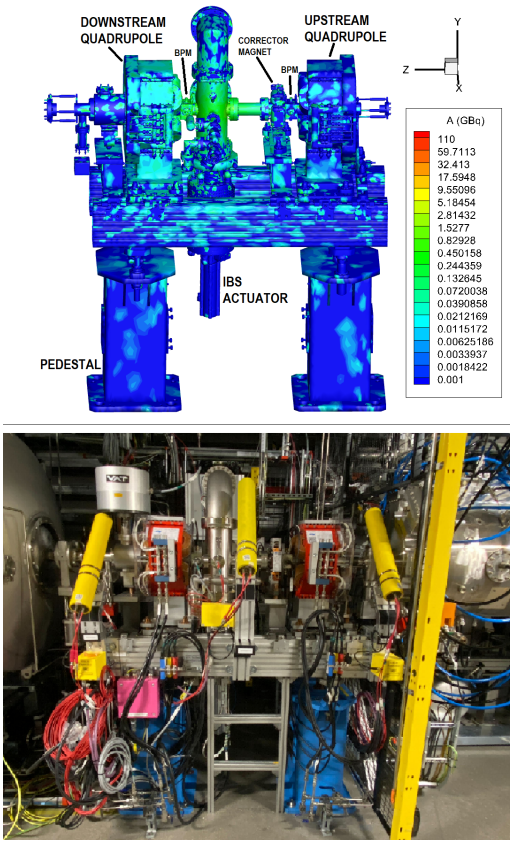

Figure 3: The first SPK section of the ESS superconducting linac: (top) Activation calculations on top of the model and (bottom) photo of the actually installed section. The dimensions in (X×Y×Z) are: (90 cm × 170 cm × 200 cm).

ISBN: 978-3-95450-262-2 ISSN: 2673-5350 doi: 10.18429/JACoW-IBIC2025-MOPMO07

were completed on the DMSC cluster, the `mctal` file was converted to the flux-to-moment file (in the .rtm format) in few seconds. For the activation calculations in Fornax, the same mesh, materials, energy group attributes, cross-sections, region attributes, MCNP controls and fixed source settings were exploited. The irradiation and decay times can be defined in subsequent steps with the appropriate normalization. This feature was particularly useful during the linac commissioning, given the frequently changes in the average proton current. An activity report is created for each step: a list of isotope is provided, along with the quantity (in atoms), the activity (in Bq), the activity density (in Bq/cm^3), the total and cumulative radionuclide percentages for each linac component. It is possible to visualize in Tecplot not only the overall activation on top of the linac model, but also the volumetric distribution for each radioisotope. In the model of Fig. 3, the main nuclide of radiological importance found in the beamp pipe is Cr-51. The quadrupole downstream the beam stop is more activated with respect to the quadrupole upstream, due to the fact that most of the secondary particles fly downstream the beam stop. The results guide routinely RP surveys, pointing out hotspots along the proton linac.

CONCLUSIONS AND OUTLOOK

The Attila4MC software is versatile, efficient and accurate for radiation transport simulations of the ESS proton linac. Representative ESS examples of the first Attila4MC simulations were described. As-built components were simulated starting directly from the CAD models, without losing time in simplifying complex linac models or manually crafting the MCNP6 geometry cell by cell. The unstructured mesh capabilities of MCNP6 were fully exploited. Attila4MC results were quickly visualized in 3D using Tecplot.

The summarized workflow for calculating the beam power density can be applied to any MCNP tally. The workflow has proven to be useful for assessing materials for key structural components before proceeding with the manufacturing of expensive components. Moreover, the Attila4MC results can be post-processed in ANSYS, thus the same models can be used for advanced instrumentation and cooling design. Sharing the same models in MCNP and ANSYS allows also to fully exploit the limited space available both inside and outside the beamline.

Attila4MC and Fornax allowed to calculate the activation in entire sections of the ESS linac, providing nuclide inventories for each linac component and identifying hotspots. In the future of the ESS linac, Attila4MC will enable a variety of radiation transport simulations, including: optimization of the ESS facility space for shielding purposes, detailed mapping of radiation damage, and radionuclide inventories for radiation waste categorization.

ACKNOWLEDGMENTS

The author is grateful to the staff at Silver Fir Software for the support during the installation of Attila4MC, the tips for debugging and the continuous software development.

The CAD models were provided by the ESS colleagues in the Mechanical Engineering Department, ESS in-kind collaborators or manufacturers all around the world. All the simulations ran on the cluster of the ESS Data Management and Software Centre (DMSC) in Copenhagen (Denmark).

REFERENCES

[1] R. Garoby *et al.*, "The European Spallation Source design", *Phys. Scr.*, vol 93, p. 014001, 2018. doi:10.1088/1402-4896/aaecea

[2] R. J. Barlow, A. M. Toader, L. Tchelidze, and H. D. Thomsen, "Background Calculations for the High Energy Beam Transport Region of the European Spallation Source", in *Proc. IPAC'14*, Dresden, Germany, Jun. 2014, pp. 2137–2139. doi:10.18429/JACoW-IPAC2014-WEPRO078

[3] D. Di Julio *et al.*, "Radiation transport calculations for the European Spallation Source accelerator environment", in *14th International Conference on Radiation Shielding and 21st Topical Meeting of the Radiation Protection and Shielding Division (ICRS 14/RPSD 2022) meeting*, Sep. 2022, pp. 423–426.

[4] L. Lari, M. Eshraqi, L. S. Esposito, L. Tchelidze, F. Cerutti, and A. Mereghetti, "FLUKA Modeling of the ESS Accelerator", in *Proc. IPAC'15*, Richmond, VA, USA, May 2015, pp. 434–437. doi:10.18429/JACoW-IPAC2015-MOPJE058

[5] Attila4MC®, https://www.silverfirsoftware.com/Pages/Products/Attila4MC.php

[6] E. Donegani *et al.*, "Design and performance of the compact DTL1 Faraday cup for the high-power ESS NCL", *Nucl. Instrum. Methods Phys. Res. A*, vol. 1047, p. 167827, 2022. doi:10.1016/j.nima.2022.167827

[7] I. Bustinduy I. Bustinduy *et al.*, "Progress on ESS Medium Energy Beam Transport", in *Proc. LINAC'14*, Geneva, Switzerland, Aug.-Sep. 2014, paper TUPP025, pp. 484–486.

[8] ANSYS, http://www.ansys.com

[9] Tecplot, Inc., Bellevue, WA, 360 EX 2018 Release 2, 2018.

[10] ANSYS SpaceClaim, www.spaceclaim.com

[11] C. Werner *et al.*, "MCNP User Manual, Code Version 6.2", Los Alamos National Laboratory, NM, USA, LA-UR-17-29981, 2017.

[12] D. B. Pelowitz Ed., "MCNPX Users Manual Version 2.7.", Los Alamos National Laboratory, NM, USA, LA-CP-11-00438, 2011.

[13] The ESS DMSC, https://europeanspallationsource.se/data-management-software-centre

[14] E. Donegani *et al.*, "Challenges with the beam destinations for the ESS linac", presented at IBIC'25, Liverpool, UK, Sep. 2025, paper MOPMO06, this conference.

[15] E. Donegani *et al.*, "Design and initial performance of the beam stop for the first spoke section of the ESS superconducting proton linac", *Nucl. Instrum. Methods Phys. Res. A*, vol. 1081, p. 170848, 2026. https://doi.org/10.1016/j.nima.2025.170848

[16] Fornax, https://www.silverfirsoftware.com/Pages/Products/Fornax.php